Front. Struct. Civ. Eng. 2017, 11(3): 360–367
DOI 10.1007/s11709-017-0429-3

RESEARCH ARTICLE

Investigation of mechanical performance of prestressed steel arch in tunnel

Yaqiong WANG[a*], Yunxiao XIN[a], Yongli XIE[a], Jie LI[b], Zhifeng WANG[a]

[a] *School of Highway, Shaanxi Provincial Major Laboratory for Highway Bridge & Tunnel, Chang'an University, Xi'an 710064, China*

[b] *Shaanxi Communication Technology Consulting Co., Ltd., Xi'an 710068, China*

[*] *Corresponding author. E-mail: wangyqchd@126.com, 250960825@qq.com*

ABSTRACT In the traditional tunneling method, the steel arch are often adopted to support surrounding rock to ensure the structural stability. If the steel arch is prestressed in time, tunnel support can effectively prevent the development of rock crack, thereby increasing the overall strength of tunnel support and suppress the deformation of the surrounding rock. Based on the mechanical model of steel arch established in this paper, the stress distribution of steel arch is investigated via the numerical simulation method, and the impact on surrounding rock is also analyzed. Through a field test, the rules of the arch strain distribution are observed and discussed. The results show that the prestressed steel arch structure can provide effective support and the stress gradually decreases from stress point to another arch springing. Furthermore, the stress distribution applied by the prestressed steel arch on the surrounding rock is uniform in a certain extent, and it is suggested that this construction method utilizing the prestressed steel arch to squeeze surrounding rock is feasible from a theoretical view.

KEYWORDS tunnel support, prestressing force, steel arch, numerical analysis

1 Introduction

As an important measure of tunnel support, steel arch plays a key role on deformation and stability of tunnel during excavation. However, the steel arch began to produce the supporting effect only when the deformation of the surrounding rock became sufficient and tight contact with arch in traditional method (as shown in Fig. 1). Based on the New Austrian Tunneling Method (NATM), some people analyzed the distribution of stress and deformation and came up with their ideas about the tunnel lining. Papanikolaou and Kappos [1] analyzed the structural response of unreinforced concrete tunnel linings with the numerical simulation. Bilotta and Russo [2] collected the force data of steel arch and observed its regularity. As for the position of structure, Dancygier et al. [3] thought that there is a certain angle of tunnel roof has the maximum pressure value by the theoretical analysis. And the deformation of lining structure near the tunnel intersection was larger than the deformations in distant sections [4].

Apart from the mechanical analysis with traditional lining, some optimized tunnel structure also be analyzed.

Fig. 1 Steel arch used in tunnel engineering

Article history: Received Feb 15, 2017; Accepted Apr 5, 2017

Such as a supporting system of grid steel frame-core tube, who could significantly control the large deformation of surrounding rock [5]. In the area of steel arch, a new U-type steel arch had a superb effect on the surrounding rock control by the application [6].

However, this kind of passive supporting method can lead to the further developing of the cracks in surrounding rock structure [7], and therefore, the strength of the whole surrounding rock and supporting structure is reduced. If we impose the prestress on tunnel support, the force state of supporting structure would change from the passive state to the active status, and it would suppress the development of the fissures of the surrounding rock and can strengthen the mechanical properties of the supporting structure.

At present, the applications of the prestressed technology in the field of tunnel are relatively narrow, and this technology is mainly used in the joint between different shield lining segments. For instance, Liu Feng-jun ever did some theoretical researches of tunnel lining segment with the prestressed joint [8]. Although there are some breakthroughs of prestressed technology in tunnel area, due to the strength limitations of these applications, prestressing technology is hardly to be adopted in tunnel support area [9–11]. Taking into account the importance of the steel arch in supporting structure, putting prestress on steel arch can achieve the aim for controlling the further damage of surrounding rock [12]. Currently, the study of the mechanical properties of steel arch in tunnel is still in the initial stage, Wen et al. analyzed the stress distribution of steel arch [13,14].

So far there is no application of prestressed technology in tunnel steel arch, based on the former research results of tunnel steel arch, this paper analyze the overall stress situation of the prestressed arch structure through the numerical simulation of mechanical model, and discuss the theoretical feasibility of prestressed steel arch by experimental measurement.

2 Mechanical model

2.1 Theoretical derivation

The mechanical homeostasis of surrounding rock is hardly maintained after tunnel excavation under adverse geological condition, so the steel arch has become a necessary part of the supporting structure, and work with shotcrete, bolt and steel mesh to improve the overall strength and rigidity of support, thereby suppressing the further deformation of surrounding rock and ensuring the quality of the whole surrounding rock belt [15–18]. Therefore, the prestressing steel arch can squeeze the surrounding rock, which will result in the improvement of the strength and stiffness of surrounding rock in some extent. Since the prestressing will be accompanied by the deformation of steel arch, the amount of prestress should be long maintained, and we must first ensure that the feet-lock bolt or inverted arch and other fixed measures are completed, and then prestress the steel arch. The principle of steel arch structure installation is shown in Fig. 2, firstly erecting the steel arch on the designated position, then assembling the steel arch and fixing the side wall of arch, only reserving a sliding part between the side wall portion and one of the arch endpoint. Then, the jack need to be used to impose prestressing force on one of an endpoint in arch, then welding the joint between the arch and sidewall when the stress value achieved the design requirement, and the installation of the prestressing steel arch is completed.

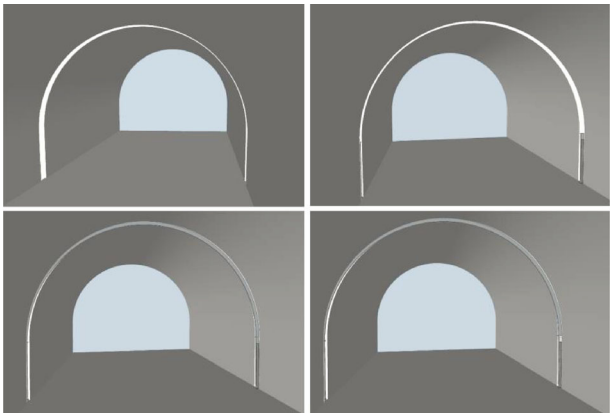

Fig. 2 Illustration of the procedure for assembling prestressed steel arch

Due to the fixation of the foot bolt lock, the prestress can only be applied in the semi-circular arch, so this paper describe the governing equations of prestressed semi-circular steel arch in the following section. Assuming that the steel arch is I-beam, and the inner and outer radius of curved beam structure are r_0 and r_1 respectively; I-beam section height is $h = r_1\text{-}r_0$; sectional area is A and section moment of inertia is I; the center radius is $r = (r_1 + r_0)/2$. Intercepting the force element $r\mathrm{d}\theta$ (as shown in Fig. 3), it can be seen that the radial displacement is $\omega(\theta)$, and K is rock resistant coefficient. The initial section bending moment is $M(\theta)$, the shear stress is $Q(\theta)$ and the axial force is $N(\theta)$. All of the force above mentioned use the direction in figures as the positive direction. The mechanical model of prestressed steel arch subject to prestress and surrounding rock is depicted in Fig. 3. It is assumed that the steel arch is I-beam, by establishing the equilibrium equations of infinitesimal segments and omitting higher order trace, and then we can get the formula:

$$\mathrm{d}Q(\theta) + N(\theta)\mathrm{d}\theta + K\omega(\theta)r_1\mathrm{d}\theta = 0, \tag{1}$$

$$Q(\theta)\mathrm{d}\theta - \mathrm{d}N(\theta) = 0, \tag{2}$$

$$\mathrm{d}M(\theta) - r\mathrm{d}N(\theta) = 0. \tag{3}$$

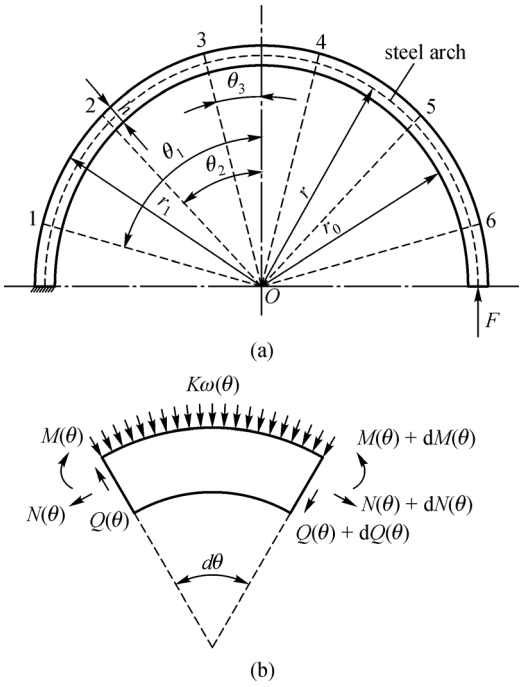

Fig. 3 Calculating diagram for circular beam on elastic foundation of steel arch. (a) Beam geometry; (b) Forces on a small beam

By the related concepts in structural mechanics, the arch radial displacement $\omega(\theta)$ has the following relationship with section internal force:

$$\frac{\mathrm{d}^2\omega(\theta)}{\mathrm{d}\theta^2}+\omega(\theta)=\frac{M(\theta)r^2}{EI}+\frac{N(\theta)r}{EA}. \tag{4}$$

Assuming that the steel arch is made by the single homogeneous material, the following equation can be derived by combing the Eqs. (1)–(4):

$$\frac{\mathrm{d}^5\omega(\theta)}{\mathrm{d}\theta^5}+2\frac{\mathrm{d}^3\omega(\theta)}{\mathrm{d}\theta^3}+n^2\frac{\mathrm{d}\omega(\theta)}{\mathrm{d}\theta}=0, \tag{5}$$

where $n^2=1+Kr_1\left(\frac{r^3}{EI}+\frac{r}{EA}\right)$, and the general solution of Eq. (5) can be listed as follows:

$$\omega(\theta)=C_0+C_1\mathrm{ch}\alpha\theta\cos\beta\theta+C_2\mathrm{sh}\alpha\theta\cos\beta\theta+C_3\mathrm{ch}\alpha\theta\sin\beta\theta+C_4\mathrm{sh}\alpha\theta\sin\beta\theta, \tag{6}$$

where $\alpha=\sqrt{\frac{n-1}{2}},\beta=\sqrt{\frac{n+1}{2}}$; C_0–C_4 are integration constant.

Combining the Eqs. (1)–(3) and (6), we can get the supporting force formula of the tunnel steel arch:

$$\begin{aligned}Q(\theta)=T[&C_1(A_1\mathrm{sh}\alpha\theta\cos\beta\theta+A_2\mathrm{ch}\alpha\theta\sin\beta\theta)\\&+C_2(A_1\mathrm{ch}\alpha\theta\cos\beta\theta+A_2\mathrm{sh}\alpha\theta\sin\beta\theta)\\&+C_3(A_1\mathrm{sh}\alpha\theta\sin\beta\theta-A_2\mathrm{ch}\alpha\theta\cos\beta\theta)\\&+C_4(A_1\mathrm{ch}\alpha\theta\sin\beta\theta-A_2\mathrm{sh}\alpha\theta\cos\beta\theta)],\end{aligned} \tag{7}$$

$$N(\theta)=-Kr_1C_0-C_1D\mathrm{sh}\alpha\theta\sin\beta\theta-C_2D\mathrm{ch}\alpha\theta\sin\beta\theta+C_3\mathrm{sh}\alpha\theta\cos\beta\theta+C_4D\mathrm{ch}\alpha\theta\cos\beta\theta, \tag{8}$$

$$\begin{aligned}M(\theta)=\frac{1}{B_2}[&(Kr_1B_1+1)C_0-C_1(B_1D-2\alpha\beta)\mathrm{sh}\alpha\theta\sin\beta\theta\\&-C_2(B_1D-2\alpha\beta)\mathrm{ch}\alpha\theta\sin\beta\theta\\&-C_3(B_1D-2\alpha\beta)\mathrm{sh}\alpha\theta\cos\beta\theta\\&+C_4(B_1D-2\alpha\beta)\mathrm{ch}\alpha\theta\cos\beta\theta],\end{aligned} \tag{9}$$

where $A_1=\alpha^3-3\alpha\beta^2+\alpha$, $A_2=\beta^3-3\alpha\beta^2-\beta$,

$$B_1=r/(EA),B_2=r^2/(EI),D=T(A_2\alpha-A_1\beta),$$

$$T=[r^3/(EI)+r/(EA)]^{-1}.$$

Tunnel section shape generally is symmetrical about its vertical axis, and the stress distribution is non-biased, so it can be assumed that the surrounding rock load is also symmetrical about its vertical axis. Therefore the section of vertical axis can be set as initial section, and the following equation can be obtained:

$$\omega(\theta)=\omega(-\theta);N(\theta)=N(-\theta). \tag{10}$$

Since C_2= C_3= 0, so the Eqs. (7)–(9) can be simplified as:

$$\begin{aligned}Q(\theta)=T[&C_1(A_1\mathrm{sh}\alpha\theta\cos\beta\theta+A_2\mathrm{ch}\alpha\theta\sin\beta\theta)\\&+C_4(A_1\mathrm{ch}\alpha\theta\sin\beta\theta-A_2\mathrm{sh}\alpha\theta\cos\beta\theta)],\end{aligned} \tag{11}$$

$$N(\theta)=-Kr_1C_0-C_1D\mathrm{sh}\alpha\theta\sin\beta\theta+C_4D\mathrm{ch}\alpha\theta\cos\beta\theta. \tag{12}$$

$$\begin{aligned}M(\theta)=\frac{1}{B_2}[&(Kr_1B_1+1)C_0-C_1(B_1D-2\alpha\beta)\mathrm{sh}\alpha\theta\sin\beta\theta\\&+C_4(B_1D-2\alpha\beta)\mathrm{ch}\alpha\theta\cos\beta\theta].\end{aligned} \tag{13}$$

In the Eqs. (11)–(13), when the integration constant C_0, C_1, C_4 can be obtained, we will further get the analytical formula of the internal force of support structure. Integration constant C_0, C_1, C_4 are usually determined by the boundary conditions at both ends of the curved beam which is generally regarded as the elastic fixed restraint.

2.2 Numerical simulation analysis

Based on the former theories, the prestressed steel arch

model is established by the finite element analysis software ABAQUS, and the internal stress distribution of the steel arch and its impact on surrounding rock are analyzed. Firstly, it is assumed that this project is normal two-lane tunnel, and surrounding rock is grade IV. In addition, for simplification, it is assumed that there is no friction between the arch and surrounding rock. The internal friction angle of surrounding rock is $\varphi = 27°$, and the cohesion is $c = 0.2$ MPa. The type of beam is I20b, the radius of arch axis is $r = 6.39$ m, and the cross-sectional area is $A = 39.55$ cm^2. The left endpoint is supported by surrounding rock, and the arch outer edge sliding contact with surrounding rock. The material parameters used in this model are shown in Table 1. The right endpoint is subjected to the vertical upward direction force with 1000 kN. The Mises criterion is used in calculation, and the process of stress distribution is observed. Fig. 4 shows the finite element mesh used in the calculation.

Table 2 shows the calculated stress of the steel arch after applying prestressing force. As can be seen, after applying 1000 kN prestressing stress, there is a maximum stress with 372 MPa near the left endpoint, and the stress gradually decreases along the arch axis. Since the maximum stress occurred in the inner edge of arch, we use the inside axis of curved beam as stress path, and observe the specific changes of the stress in this path.

Fig. 5 depicts the stress distribution of the inner side of steel arch. As shown in Fig. 5, before prestressing steel arch, the internal stress distribution is symmetrical, and the stress value of whole steel arch, especially in the central part is small, and hardly achieve the full material strength. After prestressing, the stress of steel arch reaches a peak near the force point and gradually decreases along the circumferential direction of arch. The stress distribution is significantly asymmetric, and the whole stress value of arch is larger than before. In this condition, the structure material can achieve its strength, and the overall structure strength can be ensured.

Additionally, it can be observed that the stress distribution of surrounding rock impacted by the steel arch after prestressing. As is shown in Fig. 6, apart from the stress concentration phenomenon on arch foot side, the stress distribution is roughly uniform on the other part of tunnel wall. It is suggested that the prestressing steel arch can effectively and uniformly transmit the force to tunnel wall, which can reinforce the surrounding rock belt.

3 Strain measurement

3.1 Component layout

In order to verify the reasonableness of the numerical model, this paper further analyzes the stress distribution of the prestressed steel arch through the strain measurement of steel arch in a tunnel engineering project. Taking into account the operational difficulties of measuring the stress of steel arch, this paper assumed that steel arch is working in the elastic stage throughout the test. Based on the strain measurement of the arch surface, the strain variation of arch with time can be observed, and the stress distribution of the steel arch can be indirectly analyzed according to the formula $\varepsilon = \sigma/E$. This project used I20b beam and arranged six strain cells on the lower side of beam web (as shown in

Table 1 Material parameters used in numerical model

Model	Element type	Modulus E(GPa)	Poisson ratio	Density ρ(kg/m^3)
Steel arch	I20b	206	0.3	7850
Surrounding rock	Grade IV	10	0.35	2000

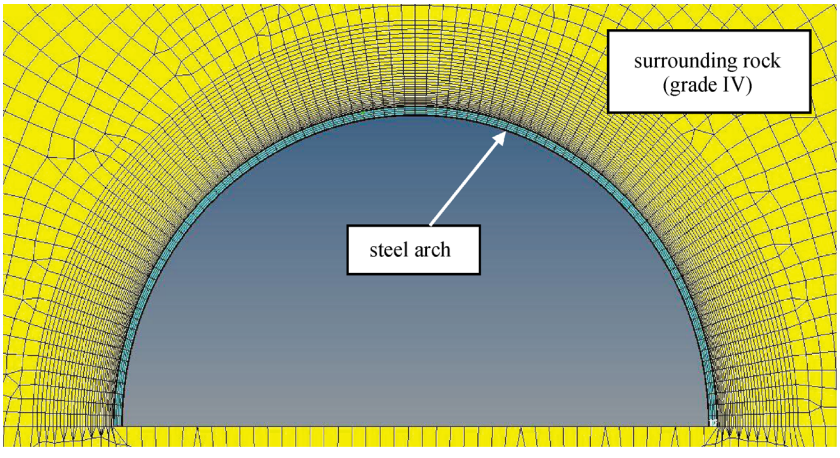

Fig. 4 Finite element mesh used in the calculation

Table 2 Calculated stress of the steel arch after applying prestressing force

L (m)	σ (MPa)	L (m)	σ (MPa)	L (m)	σ (MPa)	L (m)	σ (MPa)	L (m)	σ (MPa)
0.0	250.1	3.9	284.0	7.9	258.4	11.8	235.2	15.8	213.9
0.2	372.0	4.2	282.5	8.1	257.1	12.1	233.9	16.0	212.8
0.4	336.1	4.4	281.0	8.3	255.8	12.3	232.7	16.2	211.7
0.7	343.3	4.6	279.5	8.6	254.5	12.5	231.5	16.4	210.6
0.9	317.1	4.8	278.1	8.8	253.1	12.7	230.2	16.7	209.5
1.1	311.4	5.0	276.6	9.0	251.8	12.9	229.0	16.9	208.4
1.3	304.4	5.3	275.2	9.2	250.5	13.2	227.8	17.1	207.3
1.5	302.0	5.5	273.7	9.4	249.2	13.4	226.7	17.3	206.3
1.8	299.5	5.7	272.3	9.6	247.9	13.6	225.4	17.5	205.3
2.0	297.9	5.9	270.8	9.9	246.6	13.8	224.2	17.8	204.7
2.2	296.2	6.1	269.4	10.1	245.3	14.0	223.1	18.0	204.9
2.4	294.7	6.4	268.1	10.3	244.0	14.3	221.9	18.2	207.5
2.6	293.1	6.6	266.7	10.5	242.7	14.5	220.8	18.4	214.1
2.8	291.6	6.8	265.3	10.7	241.4	14.7	219.6	18.6	225.3
3.1	290.0	7.0	263.9	11.0	240.2	14.9	218.4	18.9	230.0
3.3	288.5	7.2	262.5	11.2	238.9	15.1	217.3	19.1	221.0
3.5	287.0	7.5	261.2	11.4	237.7	15.3	216.2	19.3	182.0
3.7	285.5	7.7	259.8	11.6	236.4	15.6	215.0	19.5	158.1

Note: L is the circumferential distance to the left endpoint of the steel arch; σ is the calculated stress by the FEM.

Fig. 2 and Table 3). After erecting the support, the strain cell on the specified position is immediately installed. When the deformation becomes stable after 5 days, the vertically upward force with 1000 kN is applied on the right arch foot, and the strain variation of the steel arc with time continued to be observed. In this study, the vibrating wire strain gauge is adopted, and the arrangement of strain gauges is shown in the Fig. 7. When the arch is under pressure, the frequency of vibration for the strain gauges can be monitored, and then the elastic strain in the steel arch can be obtained.

3.2 Test results

According to material mechanics, the elastic modulus of steel is $E = 210$ GPa, so when the strain $\varepsilon \leqslant 2000\mu\varepsilon$, the steel arch can be maintained in elastic deformation stage; while the strain $\varepsilon > 2000\mu\varepsilon$, the arch changes from the elastic deformation stage to the yield stage. Since the maximum compressive strain is $-1400\mu\varepsilon$ and the following measured data turn to stable, it can be deduced that the stress of the whole arch did not reach the yield limit. Therefore, there is an approximate linear relationship between the stress and strain of the steel arch, and the strain variation can reflects the changes of stress distribution indirectly.

As shown in Fig. 8, the strain of the steel arc is mainly in the compression state, and the initial strain values are fluctuant. Because of the absence of prestressing, this chart mainly shows the initial deformation and the adjustment status of conventional steel arch in first 5 days. When we apply the force in the 5th day, there is a surge of strain near the force point, and this variation trend became slow after 10th day. Several fluctuations in the graph may be caused by the blasting during excavation. From the strain distribution chart, it can be found that the strain value of arch gradually decrease from the force point to another arch endpoint. Near the force point there will be the greater value of strain, but for the remaining parts of arch the strength properties can be fully used in elastic stage. It is shown that the strain distribution of whole arch in this test is approximately similar to the stress distribution in the former numerical simulation.

4 Conclusion

In order to fully exert the structure strength and reduce the further damage to the surrounding rock, the prestressing steel arch is adopted to squeeze surrounding rock. In this paper, the corresponding mechanical model of the prestressing steel arch is established to analyze the feasibility of this kind of working method in theory. Based on the analysis of mechanical properties and stress state for prestressed steel arch, this paper set steel arch structure as an elastic beam and the theoretical formulas for the internal stress of steel arch is also derived. Meanwhile, this paper also investigated the stress distribution of

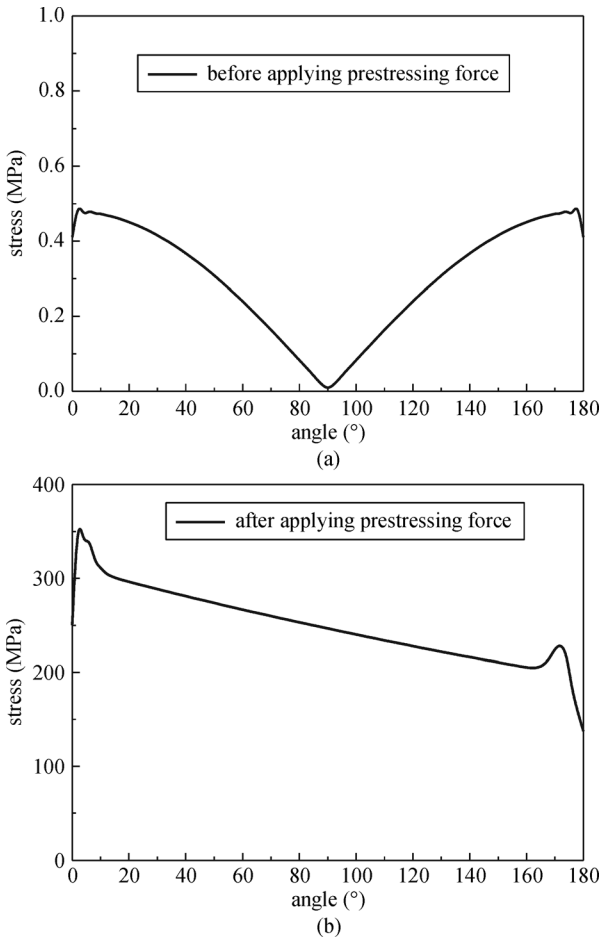

Fig. 5 Stress distribution of the inner side of steel arch. (a) Before applying prestressing force; (b) After applying prestressing force

prestressed steel arch and its effect on the surrounding rock combining the numerical simulation results with the strain measurement. The following conclusions can be drawn:

(1) Prestressing steel arch in tunnel can be adopted to exert the mechanical properties of the support structure, and make full use of the material strength.

(2) The maximum value of stress occurs in the arch inside near the force point, and this part should be strengthened or replaced by high-strength material to ensure the strength and stability of the whole structure when applying more pressure on the arch.

(3) The stress distribution of surrounding rock is roughly uniform, and the arch can transmit the stress to surrounding rock in the contact interface. A compressive stress zone can be formed in surrounding rock. The surrounding rock belt can be effectively strengthened to avoid the further development of cracks in surrounding rock.

(4) Although the simulation results indicates that there exists the stress concentration phenomena in arch foot, taking into account that the arch is not just standing on surrounding rock in practical projects, and the invert arch and feet-lock bolt are also involved in the action, therefore the stress concentration phenomena may be ignored.

(5) The results show that the prestressed steel arch used to reinforce the surrounding rock belt is feasible from a theoretical view. However, this article just considered the main factors such as stress and strain in the process of establishing the mechanical model, and did not consider other factors such as stability, therefore the application of this construction method need to be confirmed further in practical engineering project.

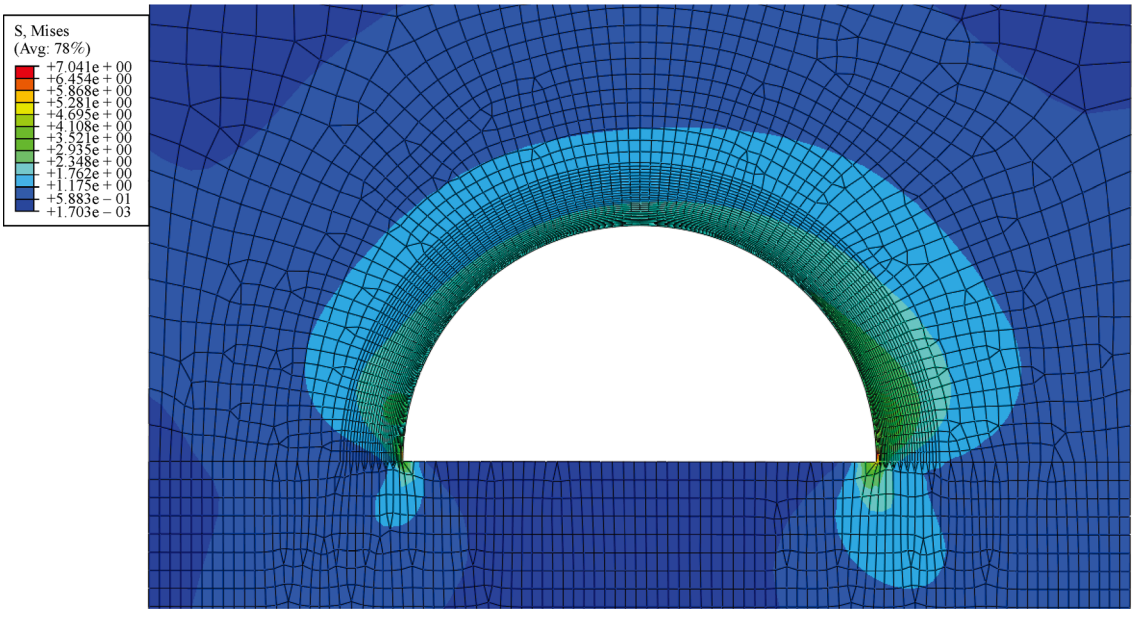

Fig. 6 Stress distribution cloud chart of surrounding rock

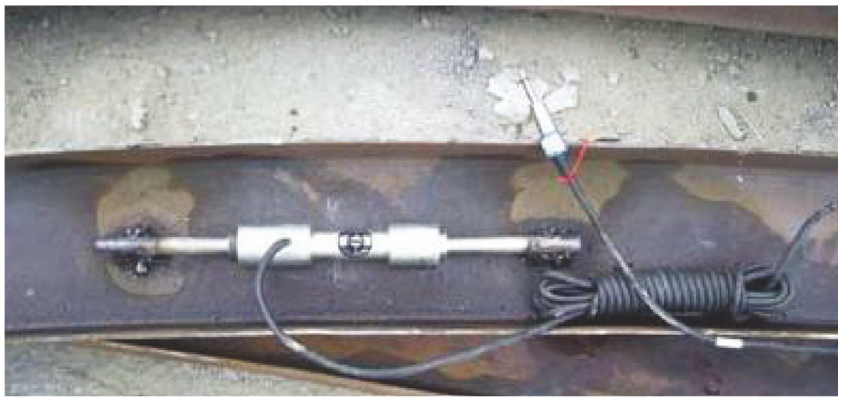

Fig. 7 Strain gauges installed in field

Table 3 Arrangement of Strain Cells on Arch

Number	1#	2#	3#	4#	5#	6#
Horizontal angle	15°	45°	75°	105°	135°	165°
Position	foot	lumbar	vault	vault	lumbar	foot

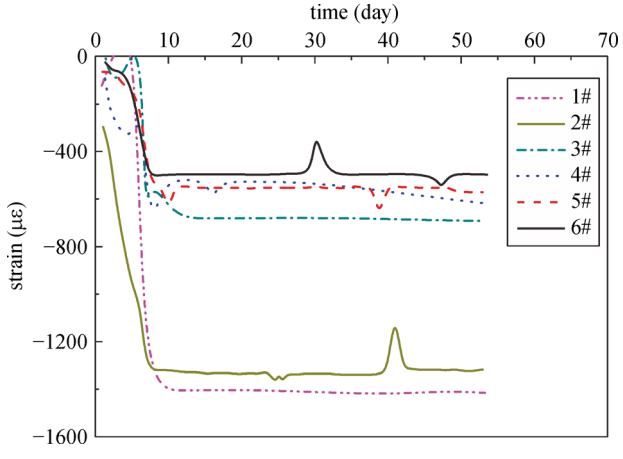

Fig. 8 Strain variation chart of the steel arc support

Acknowledgements The research work described herein was funded by the Fundamental Research Funds for the Central Universities (310821153312 & 310821161022), China Postdoctoral Science Foundation. These financial supports are gratefully acknowledged.

References

1. Papanikolaou V K, Kappos A G. Practical nonlinear analysis of unreinforced concrete tunnel linings. Tunnelling and Underground Space Technology, 2014, 40(1): 127–140
2. Bilotta E, Russo G. Lining structural monitoring in the new underground service of Naples (Italy). Tunnelling and Underground Space Technology, 2016, 51(5): 152–163
3. Dancygier A N, Karinski Y S, Chacha A. A model to assess the response of an arched roof of a lined tunnel. Tunnelling and Underground Space Technology, 2016, 56: 211–225
4. Li Y Y, Jin X G, Lv Z T, Dong J H, Guo J C. Deformation and mechanical characteristics of tunnel lining in tunnel intersection between subway station tunnel and construction tunnel. Tunnelling and Underground Space Technology, 2016, 56: 22–33
5. Xu F, Li S C, Zhang Q Q, Li L P, Shi S S, Zhang Q. A new type support structure introduction and its contrast study with traditional support structure used in tunnel construction. Tunnelling and Underground Space Technology, 2017, 63: 171–182
6. Wang Q, Jiang B, Li S C, Wang D C, Wang F Q, Li W T, Ren Y X, Guo N B, Shao X. Experimental studies on the mechanical properties and deformation & failure mechanism of U-type confined concrete arch centering. Tunnelling and Underground Space Technology, 2016, 51: 20–29
7. Wei Y, Wang Y Q, Gao X. Effect of Internal Curing on Moisture Gradient Distribution and Deformation of a Concrete Pavement Slab Containing PreWetted lightweight Fine Aggregates. Drying Technology, 2015, 33(3): 355–364
8. Liu F J. Study on the design philosophy of prestressed concrete linings for shield tunnel. Tongji University, Doctor Degree Thesis, Shanghai, 2007
9. Lai J X, Fan H B, Chen J X, Qiu J L, Wang K. Blasting vibration monitoring of undercrossing railway tunnel using wireless sensor network. International Journal of Distributed Sensor Networks, 2015, 11(6): 703980
10. Wang K Z, Liu Y R, Wang Y P. Study of deformation characteristics of compound support steel arch and surrounding rock stability in diversion tunnel. Chinese Journal of Rock Mechanics and Engineering, 2014, 33(2): 217–224
11. Wang W X, Zhao W S, Huang L X, Vimarlund V, Wang Z W. Applications of terrestrial laser scanning for tunnels: a review. Journal of Traffic and Transportation Engineering, 2014, 1(5): 325–337

12. Xue W J, Wang D, Wang L B. A Review and Perspective about Pavement Monitoring. International Journal of Pavement Research and Technology, 2012, 5(5): 295–302
13. Wen J Z, Zhang Y X, Wang C. Back analysis of internal force of initial support in tunnel based on touch stress. Rock and Soil Mechanics, 2011, 32(8): 2467–2472
14. Wen J Z, Zhang Y X, Wang C. Back analysis for the mechanical properties of initial tunnel support based on steel arch stresses. China Civil Engineering Journal, 2012, (2): 170–175
15. Shen C H, Tong L Y. Dscussions on predicting the stability of flexible shotcrete and steel arch frame support for tunnels. China Civil Engineering Journal, 2007, 40(3): 88–91
16. Lai J X, Mao S, Qiu J L, Fan H B, Zhang Q, Hu Z N, Chen J X. Investigation progresses and applications of fractional derivative model in geotechnical engineering. Mathematical Problems in Engineering, 2016, 3: 1–15
17. Wen J Z. Study on mechanical analysis of tunnel initial support and its parameters optimization. Doctor Degree Thesis, Chongqing University, Chongqing, 2012
18. Xu H, Li T B, Xia L, Zhao J X, Wang D. Shaking table tests on seismic measures of a model mountain tunnel. Tunnelling and Underground Space Technology, 2016, 60: 197–209